ISSN 0021-3640, JETP Letters, 2020, Vol. 111, No. 7, pp. 397–402. © Pleiades Publishing, Inc., 2020.
Russian Text © The Author(s), 2020, published in Pis'ma v Zhurnal Eksperimental'noi i Teoreticheskoi Fiziki, 2020, Vol. 111, No. 7, pp. 469–474.

CONDENSED MATTER

Study of a New Type of Corrugated Nanotubes Cut out of Twisted Bilayer Graphene with the Moiré Angle Θ = 27.8°

V. A. Demin[a, *], A. A. Artyukh[a], V. A. Soroko[b, c], and L. A. Chernozatonskii[a]

[a] *Emanuel Institute of Biochemical Physics, Russian Academy of Sciences, Moscow, 119334 Russia*

[b] *Institute for Nuclear Problems, Belarusian State University, Minsk, 220030 Belarus*

[c] *Center for Quantum Spintronics, Department of Physics, Norwegian University of Science and Technology, Trondheim, NO-7491 Norway*

**e-mail: victordemin88@gmail.com*

Received March 5, 2020; revised March 5, 2020; accepted March 5, 2020

New quasi-one-dimensional hollow nanostructures similar to flattened nanotubes are numerically simulated. These nanostructures can be obtained by connecting the edges of nanoribbons cut out of twisted bilayer graphene with the Moiré angle Θ = 27.8°. The resulting nanotubes are non-chiral and contain chains of topological defects at the connected edges. A detailed description of their structure is given, and their energy stability is also demonstrated. The electronic characteristics of such structures and their evolution in the course of deformation are determined using ab initio methods. All nanotubes under study are metallic, except the structure with a width of 14 Å, characterized by the band gap $E_g = 0.2$ eV. It is shown that the electronic and elastic characteristics of such nanotubes differ significantly from those of nanoribbons forming them and of single-walled carbon nanotubes.

DOI: 10.1134/S0021364020070048

INTRODUCTION

Carbon nanomaterials, such as carbon nanotubes (CNTs) and graphene-based structures, are of considerable interest for applications because of their unique properties. One of the promising areas is their implementation in electronics. It is well known that CNTs exhibit a wide range of electronic characteristics ranging from the metallic behavior to semiconducting one with the characteristic band gaps up to 2 eV. The structure of a nanotube is characterized by indices n and m, the difference of which determines its electronic properties. If the difference $n - m$ is a multiple of three, then CNTs are metals, and for other values n and m, they are semiconductors. Carbon nanotubes were first identified in 1991 [1]. Since then, the methods of their production have become much better. However, one of the most important problems for the application of CNTs is the complexity of the synthesis of CNTs having the necessary geometry and, therefore, well-defined characteristics.

In 2013, nanotubes made of bilayer graphene with the AA packing were prepared in experiment [2]. Using transmission electron microscopy, a bilayer nanowire of a given width was cut out and its edges were then connected upon further interaction with electrons, thus forming a single-wall CNT. This technique allowed obtaining nanotubes of about 1 nm in diameter by connecting two arrays of bilayer graphene. Bilayer graphene can have AA and AB types of layer packing, and the layers can have different crystallographic orientations, i.e., be rotated by the Moiré angle Θ. The AB packing is the most stable; however, it is already possible to obtain bilayers with the Moiré angle specified with an accuracy up to 0.1°, but only slightly differing in energy stability from AB graphene [3]. The rotation of the bigraphene layers a through an angle Θ results in the formation of a superlattice with the period depending on the rotation angle [4]. The commensurate superlattice with Θ = 27.8° (Fig. 1a), which has a relatively small supercell (the number of atoms $N = 52$ and the lattice period $l = 8.9$ Å), was observed in experiment at the surface of SiC [5]. Currently, much attention is focused on Moiré bilayers because of the observation of superconductivity at 1.7 K [6]. In addition to varying the angle, various other modifications of bilayers changing their properties are possible such as physical effects changing the geometry (mechanical deformations) and structural effects (creation of holes [7–11]).

In this work, we study the structure and properties of a new type of non-chiral nanotubes, which are formed using nanoribbons obtained by cutting twisted

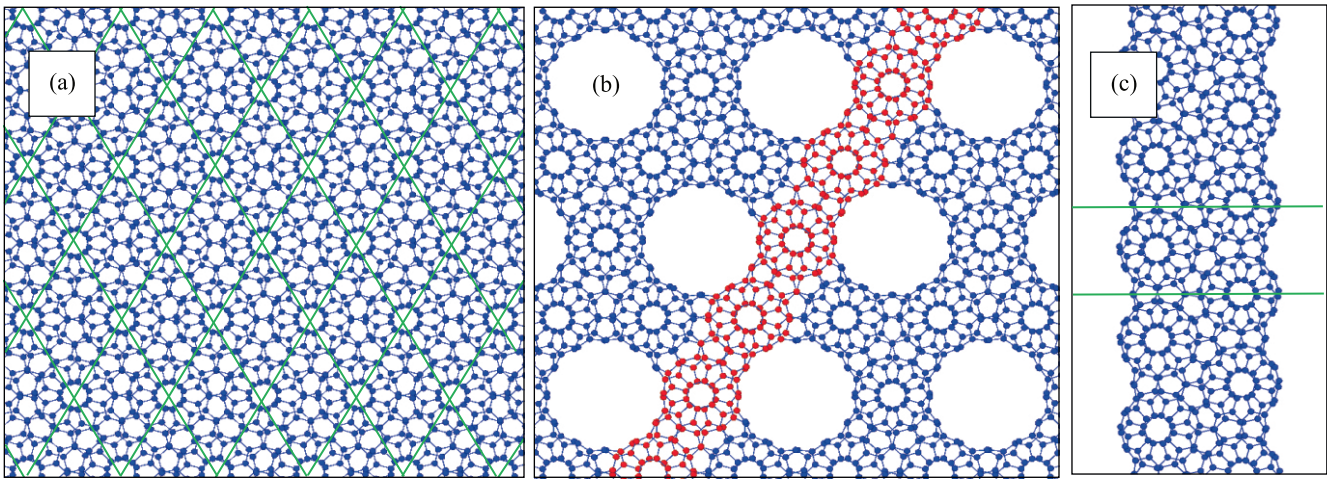

Fig. 1. (Color online) (a) Twisted bilayer graphene with the Moiré angle $\Theta = 27.8^{\circ}$ having 52 carbon atoms in the supercell. (b) Nanomesh formed by Y-shaped junctions including a one-dimensional 1FCNT array (highlighted in red). (c) 2FCNT.

bilayer graphene characterized by the Moiré angle $\Theta = 27.8°$.

CALCULATION TECHNIQUE

The calculations were performed using the SIESTA package [12] implementing the density functional theory (DFT) in the local density approximation (LDA). For the optimization of the geometry of the structures under study, the Brillouin zone was divided according to the Monkhorst–Pack method with the density of k points equal to 0.08 Å^{-1}. The distance between periodic images of quasi-one-dimensional structures exceeded 20 Å to exclude the interaction between them. The geometry of the structures was optimized to minimize the force acting on each atom down to 10^{-4} eV/Å.

RESULTS AND DISCUSSION

Earlier, we studied nanomeshes based on such a bilayer with the Moiré angle $\Theta = 27.8°$ [14]. The bilayer has characteristic circular regions, where atoms of different layers are located almost on top of each other; so, if the edge of bigraphene coincides with the boundary of the region, the layers can be connected in a manner characteristic of zigzag edges [15]. Cutting out periodically arranged round holes and then connecting the edge atoms belonging to different layers, we obtain an array of Y-shape junctions (Fig. 1b). Such a nanomesh can be represented as an array of intersecting quasi-one-dimensional structures with corrugated edges similar to compressed nanotubes (the smallest possible one is highlighted in red in Fig. 1b). Thus, it is possible to cut such corrugated nanotubes of different widths that contain n possible structures. For example, in Figs. 1b and 1c, we show the nanotubes with $n = 1$ and 2, respectively. We refer to such flattened carbon nanotube as nFCNT. The edges of the nanotube with an even n value are asymmetric.

Let us consider in more detail the 1FCNT, which is the smallest of such structures (Fig. 2a). It is a one-dimensional chain of circular regions, each containing 48 atoms (highlighted in red in Fig. 2) connected by necks including four atoms. The unit cell of such structure contains $N = 52$ carbon atoms and its lattice constant is $l = 8.8$ Å. The nFCNT consists of two asymmetric nanoribbons with chevron-type edges, which, when connected, form two pentagonal and two heptagonal defects (Fig. 2b). An increase in the width by adding 1 to n increases by 52 the number of atoms in the supercell. The nanotubes obtained are similar to chains of covalently bonded C_{60} or C_{58} fullerenes forming a one-dimensional array [16].

The DFT method was used to optimize the structure of nFCNTs with $n = 1–5$. The nanotubes with $n \geq 2$ contain a flat section, similar to that characteristic of flattened CNTs with the diameter exceeding 50 Å [17]. The calculation of the energy demonstrates that the $E/N(n)$ curve is above the energy of twisted bilayer graphene with $\Theta = 27.8°$ and tends to it with the increase in n (Fig. 2c). This behavior occurs because the ratio of the number of atoms belonging to the flat part of the nanotube to the number of atoms forming pentagonal and heptagonal defects increases with n. However, despite the defect structure of nFCNT arrays, their energy is lower than that of nanotubes with a similar perimeter: for example, the energy of CNT (3.3) is 0.03 eV/atom higher than the energy of 1FCNT.

The nFCNT consists of connected chevron-type nanoribbons (Fig. 3a). Such nanoribbons are synthesized by the self-assembly of molecules on a substrate [18]. At a width of 7.5 Å, they are semiconductors with

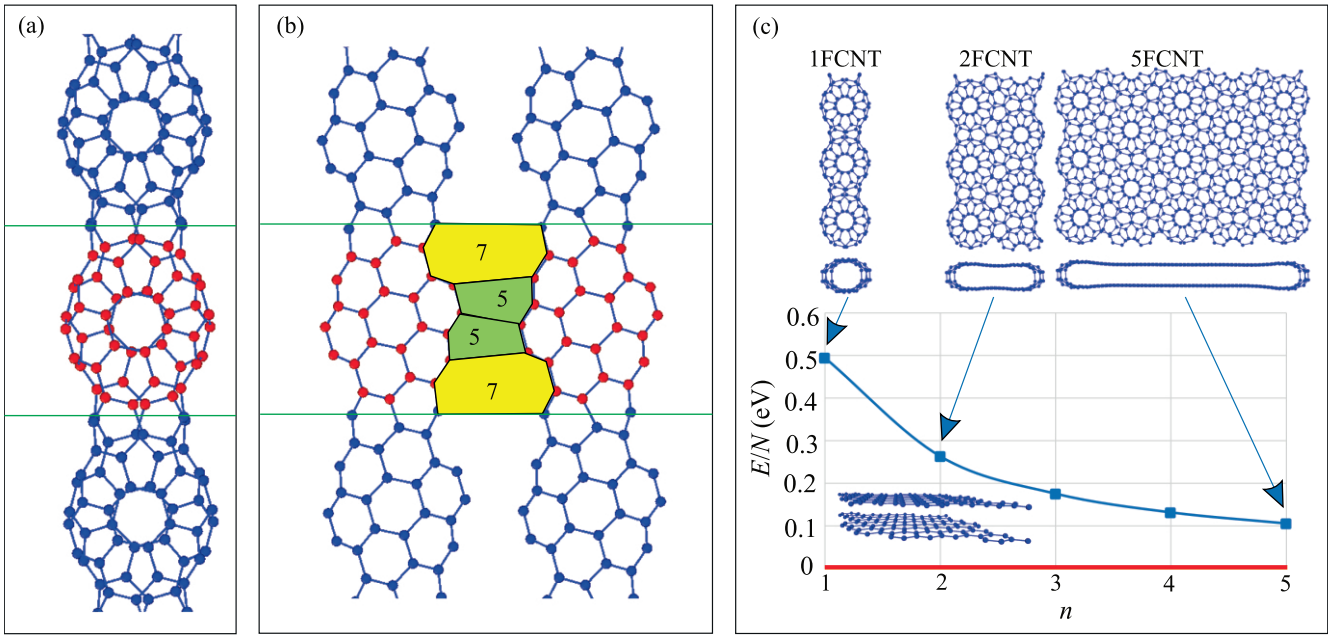

Fig. 2. (Color online) (a) Model of the *n*FCNT. (b) Unfolded nanoribbon with interlayer bonds forming two pentagonal and two heptagonal defects (7557). Green lines indicate the supercell. (c) Energy of the structure per atom measured from the energy of twisted bilayer graphene with the twist angle $\Theta = 27.8°$ versus the width of the structure.

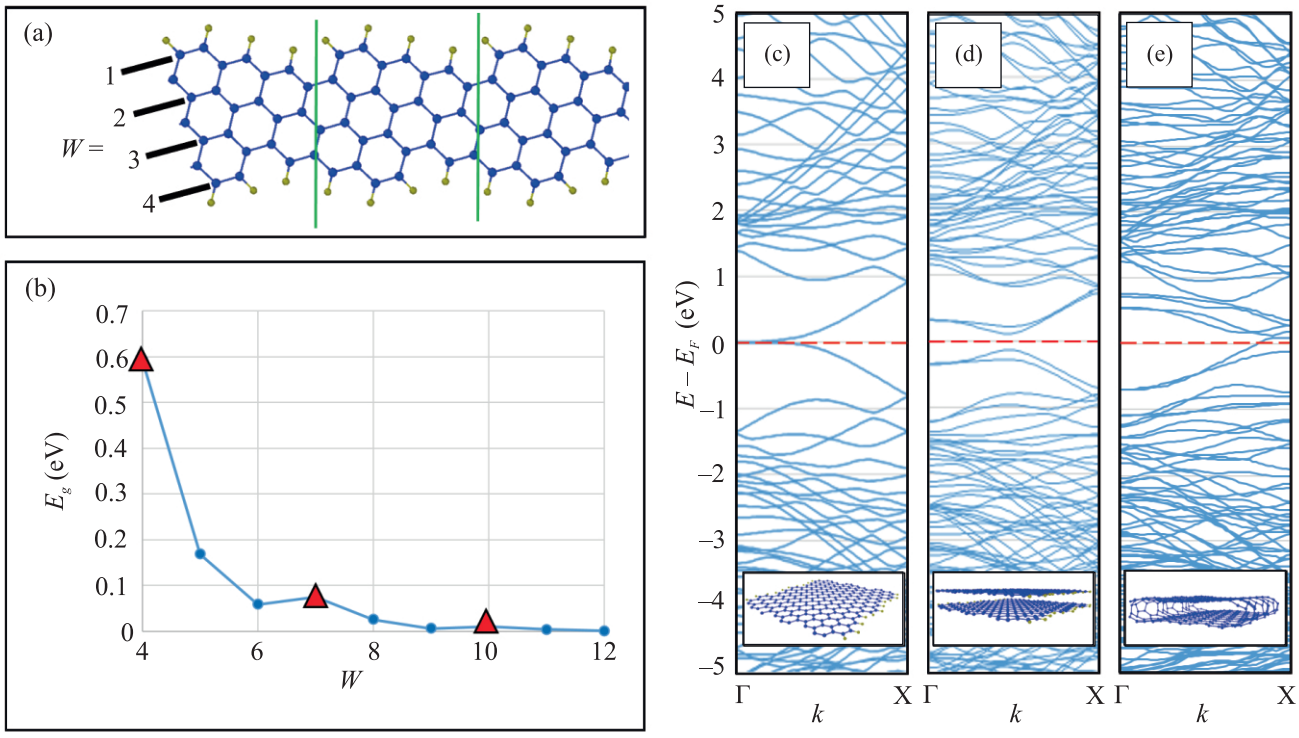

Fig. 3. (Color online) (a) 1FCNT structure including two nanoribbons with the width $w = 4$. (b) Band gap of single-layer nanoribbons versus the width w; red triangles denote the points corresponding to the nanoribbons forming the *n*FCNT. (c–e) Electronic band structures of (c) monolayer nanoribbon with $w = 7$, (d) bilayer nanoribbon, and (e) 3FCNT.

the band gap E_g = 0.3 eV [19]. In the nanoribbons studied in our work, the number of carbon atoms in the supercell is less by two. The width of such nanoribbons is characterized by the parameter w, as shown in Fig. 3a. The band gap calculated by the tight-binding method for the set of nanoribbons with w ranging from 4 to 12 is illustrated in Fig. 3b. At the minimum width equal to 7.5 Å, these nanoribbons are also semiconductors with E_g = 0.59 eV. An increase in the width leads to a rapid decrease in the band gap with insignificant oscillations, and E_g becomes less than 0.01 eV at $w \geq 11$. The overlapping of such ribbons changes the character of the band structure: all bilayer ribbons under study exhibit the band gap $E_g \sim 0.1$ eV (Fig. 3d).

The DFT-LDA calculations demonstrate that the connection of the edges of a bilayer nanoribbon leads to vanishing of the band gap in nFCNTs. An example of the evolution of the band structure, monolayer nanoribbon → a bilayer nanoribbon → nFCNT, is represented in Figs. 3c–3e. Thus, the conductivity type is independent of the width of nanoribbons under study, in contrast to conventional CNTs. However, the band gap in the 2FCNT structure is E_g = 0.2 eV. We attribute this to the existence of a planar region in such a structure comparable in size to semiconductor nanoribbons with $w \leq 7$, in contrast to the situation with 1FCNT, which has no planar regions at all, and to nFCNTs ($n \geq 3$), where the planar region does not correspond to the range of existence for semiconductor nanoribbons.

To determine Young's moduli Y, the calculations were performed with the superlattice constant varying in the range from −5% to +5% relative to its value corresponding to the state most favorable in energy. The moduli were calculated by the standard formula using data on the strain dependence of the total energy of the system [20]. The existence of pentagonal and heptagonal defects at the edges of the structures under study leads to a lower elasticity of such nanotubes compared to CNTs with the same perimeter. The smallest modulus Y = 0.6 TPa corresponds to the 1FCNT structure, for which the Young's modulus is equal to 60% of those for CNT (4.4) and CNT (7.0) having a similar perimeter. Then, the modulus Y for nFCNT increases with the index n and tends to the value Y_{graph} characteristic of graphene. Compressive/tensile strains affect the band structure of nFCNT nanotubes. In Fig. 4, we show the band structures of 4FCNT at strains of −5% and +5% in comparison to the band structure of an undistorted nanotube. At a compressive strain of 3%, the branches of the band structure near the Fermi level become separated, forming the band gap E_g = 0.13 eV. The further compression to 5% leads to an increase in this gap to E_g = 0.18 eV. The tensile strain also opens the band gap with the width smaller than 0.1 eV. In Fig. 4d, we illustrate the strain dependence of the difference ΔE between the energy levels of the valence band closest to the Fermi level and of the conduction band at the Γ point of the Brillouin zone. We can see that strains $\varepsilon \leq 3\%$ of corrugated nanotubes with indices $n \geq 3$ hardly affect ΔE: it varies within a range narrower than 0.01 eV. A strain of ε = 5% leads to approaching of the levels to each other down to 0.05 eV at the Γ point. For 2FCNT, ΔE behaves similarly, but its change is more pronounced and ΔE achieves 0.1 eV at $\varepsilon = \pm 5\%$. In 1FCNT, ΔE decreases monotonically

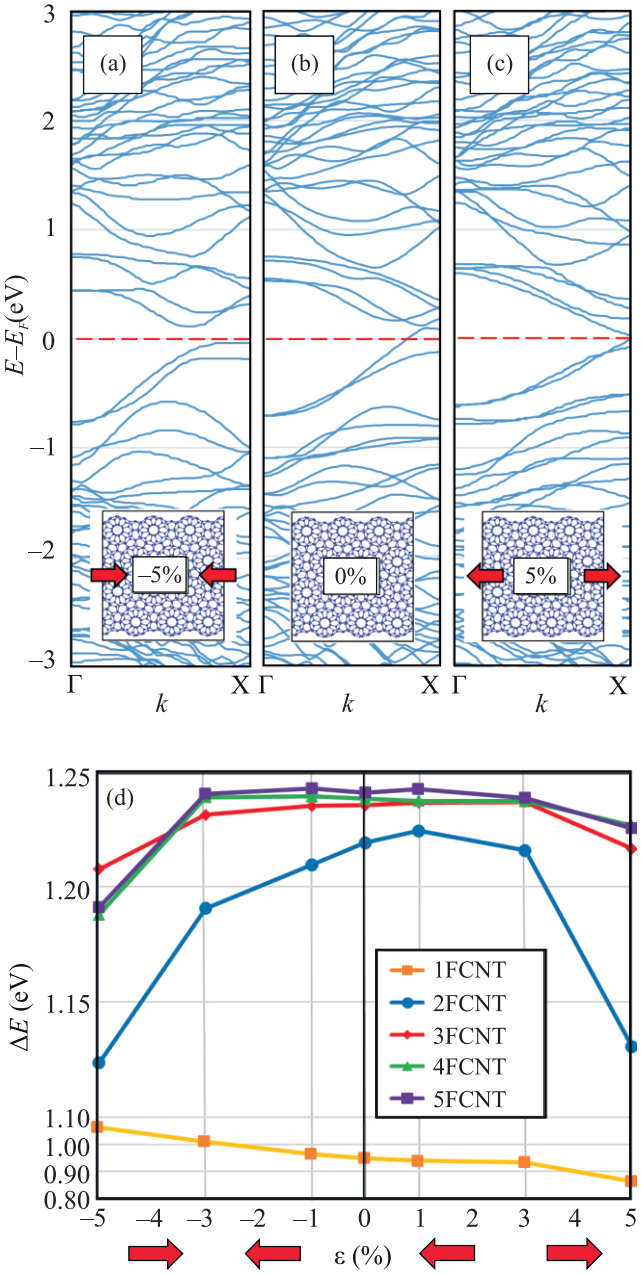

Fig. 4. (Color online) Band structure of 4FCNT (a) at a compressive strain of 5%, (b) without strain, and (c) at a tensile strain of 5%. (d) Strain dependence of the difference ΔE between the energy levels of the valence and conduction bands nearest to the Fermi level at the Γ point of the Brillouin zone.

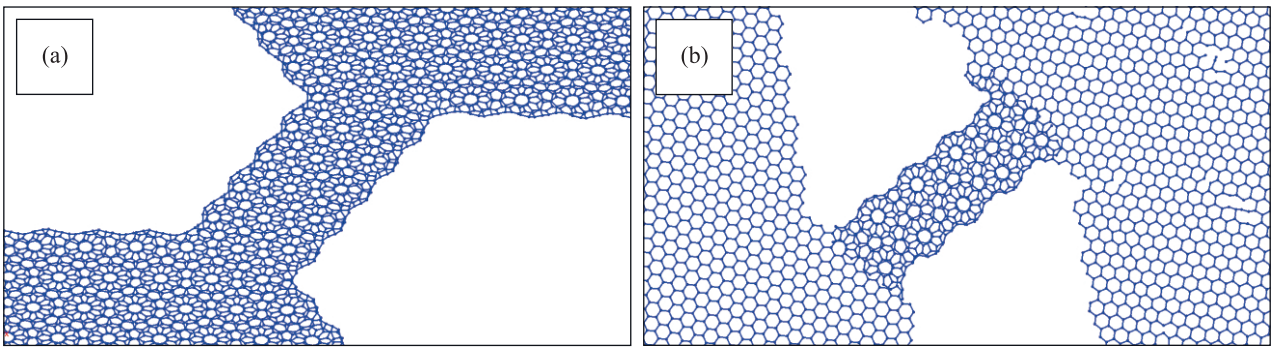

Fig. 5. (Color online) (a) Conducting 3FCNT connecting two bigraphene arrays with $\Theta = 27.8°$. (b) 2FCNT connecting two graphene monolayers with different orientations.

by 0.2 eV when the strain varies from $\varepsilon = -5\%$ to $\varepsilon = 5\%$. The stable behavior of the spectral branches at $n \geq 3$ is related to the decrease in the effect of the edges with defects on the band structure of corrugated *n*FCNTs.

We believe that such structures can be useful for applications in nanoelectronics as conducting channels between two arrays of bilayer graphene (Fig. 5a). Depending on the width of this channel, its electrical conductivity changes, in much the same way as that in folded graphene nanochannels [21], where the channel was burned out by the laser in a graphene monolayer until achieving a specified electrical resistance. Such nanotubes can also be used as crossover regions between two differently oriented graphene monolayers (Fig. 5b).

CONCLUSIONS

To summarize, we have analyzed a new class of corrugated nanotubes (*n*FCNT), which can be prepared using twisted bilayer graphene with the Moiré angle $\Theta = 27.8°$. Their structure has been described in detail and the stability of their energy state has been demonstrated. The Young's moduli have been determined; these moduli turn out to be lower than those characteristic of armchair and zigzag CNTs with a similar size owing to the presence of defects. It has been shown that the formation of such a nanotube by connecting the edges of a bilayer nanoribbon is accompanied by a significant change in its electronic band structure.

ACKNOWLEDGMENTS

The HPC computing resources at the Moscow State University [22] and at the Joint Supercomputer Center, Russian Academy of Sciences, were used.

FUNDING

This work was supported by the Russian Foundation for Basic Research (project no. 18-32-01009) and partially by the Research Council of Norway Centre of Excellence (project no. 262633, "QuSpin").

REFERENCES

1. S. Iijima, Nature (London, U. K.) **354**, 56 (1991).
2. G. Algara-Siller, A. Santana, R. Onions, M. Suyetin, J. Biskupek, E. Bichoutskaia, and U. Kaiser, Carbon **65**, 80 (2013).
3. K. Kim, M. Yankowitz, B. Fallahazad, S. Kang, H. C. P. Movva, S. Huang, S. Larentis, C. M. Corbet, T. Taniguchi, K. Watanabe, S. K. Banerjee, B. J. LeRoy, and E. Tutuc, Nano Lett. **16**, 5968 (2016).
4. J. M. Campanera, G. Savini, I. Suarez-Martinez, and M. I. Heggie, Phys. Rev. B **75**, 235449 (2007).
5. J. Hass, F. Varchon, J. E. Millan-Otoya, M. Sprinkle, N. Sharma, W. A. de Heer, C. Berger, P. N. First, L. Magaud, and E. H. Conrad, Phys. Rev. Lett. **100**, 125504 (2008).
6. Y. Cao, V. Fatemi, S. Fang, K. Watanabe, T. Taniguchi, E. Kaxiras, and P. Jarillo-Herrero, Nature (London, U.K.) **556**, 43 (2018).
7. Y. Zhang, T.-T. Tang, C. Girit, Z. Hao, M. C. Martin, A. Zettl, M. F. Crommie, Y. R. Shen, and F. Wang, Nature (London, U. K.) **459**, 820 (2009).
8. L. A. Chernozatonskii, V. A. Demin, and A. A. Artyukh, JETP Lett. **99**, 309 (2014).
9. D. G. Kvashnin, P. Vancsó, L. Yu. Antipina, G. I. Mark, L. P. Biró, P. B. Sorokin, and L. A. Chernozatonskii, Nano Res. **8**, 1250 (2015).
10. L. A. Chernozatonskii, V. A. Demin, and Ph. Lambin, Phys. Chem. Chem. Phys. **18**, 27432 (2016).
11. R. Petersen and T. G. Pedersen, J. Phys.: Condens. Matter **27**, 225502 (2015).
12. J. M. Soler, E. Artacho, J. D. Gale, A. Garcia, J. Junquera, P. Ordejón, and D. Sánchez-Portal, J. Phys.: Condens. Matter **14**, 2745 (2002).
13. H. J. Monkhorst and J. D. Pack, Phys. Rev. B **13**, 5188 (1976).
14. L. A. Chernozatonskii and V. A. Demin, JETP Lett. **107**, 315 (2018).
15. D. Zhan, L. Liu, Y. N. Xu, Z. H. Ni, J. X. Yan, C. Zhao, and Z. X. Shen, Sci. Rep. **1**, 00012 (2011).

16. E. G. Gal'pern, I. V. Stankevich, A. L. Chistyakov, and L. A. Chernozatonskii, Fullerene Sci. Technol. **6**, 499 (1998).
17. M. He, J. Dong, K. Zhang, F. Ding, H. Jiang, A. Loiseau, J. Lehtonen, and E. I. Kauppinen, ACS Nano **8**, 9657 (2014).
18. F. Schulz, P. H. Jacobse, F. F. Canova, J. van der Lit, D. Z. Gao, A. van den Hoogenband, P. Han, R. J. M. Klein Gebbink, M.-E. Moret, P. M. Joensuu, I. Swart, and P. Liljeroth, J. Phys. Chem. C **121**, 2896 (2017).
19. V. A. Saroka, H. Abdelsalam, V. A. Demin, D. Grassano, S. A. Kuten, A. L. Pushkarchuk, and O. Pulci, Semiconductors **52**, 1890 (2018).
20. A. A. Artyukh and L. A. Chernozatonskii, JETP Lett. **109**, 472 (2019).
21. I. Silvestre, A. W. Barnard, S. P. Roberts, P. L. McEuen, and R. G. Lacerda, Appl. Phys. Lett. **106**, 153105 (2015).
22. Vl. V. Voevodin, S. A. Zhumatii, S. I. Sobolev, A. S. Antonov, P. A. Bryzgalov, D. A. Nikitenko, K. S. Stefanov, and Vad. V. Voevodin, Otkryt. Sist. **7**, 36 (2012). https://www.osp.ru/os/2012/07/13017641/.

Translated by K. Kugel

SPELL: OK